Atmospheric Environment 336 (2024) 120728

Contents lists available at ScienceDirect

Atmospheric Environment

journal homepage: www.elsevier.com/locate/atmosenv

Assessing the oxidative potential of dust from great salt Lake

Reuben Attah [a,*], Kamaljeet Kaur [a], Kevin D. Perry [b], Diego P. Fernandez [c], Kerry E. Kelly [a]

[a] Department of Chemical Engineering, University of Utah, United States
[b] Department of Atmospheric Sciences, University of Utah, United States
[c] Department of Geology and Geophysics, University of Utah, United States

HIGHLIGHTS

- The GSL has reached historically low levels.
- As And Li levels in GSL exceeded EPA residential regional screening levels.
- The oxidative potential (OP) of dust from GSL is higher than the OP in other regions.
- The OP of the GSL dust was associated with metals, including Cu, Mn, Fe, and Al.
- The choice of OP assay and extraction solvent affects the OP activity of redox-active species.

ARTICLE INFO

Keywords:
Great salt lake
Particulate matter
Toxic dust
Acellular assay
Oxidative potential
Health effects

ABSTRACT

Great Salt Lake (GSL) is one of the world's largest inland bodies of saltwater. Climate change, drought, and water diversions have led to the GSL reaching historically low levels, exposing over 1945 km^2 of lakebed. Dust events can transport particulate matter (PM) from the GSL's exposed lakebed to the adjacent urban areas, presenting air quality and health concerns. In this study, we assessed the oxidative potential (OP) of dust from the exposed GSL bed compared to dust samples collected from other regional playas and to reference Arizona test dust. The oxidative potential of PM_{10} (particles ≤10 μm in aerodynamic diameter) derived from these dusts was assessed by two acellular assays: the ascorbic acid (OP^{AA}) and dithiothreitol (OP^{DTT}) and two extraction solvents: phosphate buffer saline and Gamble's simulated lung fluid. All samples were also analyzed for elemental composition. Our results show that the concentration of As and Li in most of the GSL dust samples exceeded the Environmental Protection Agency (EPA) soil residential regional screening levels, and the OP^{AA} and OP^{DTT} of dust samples from GSL playas were generally higher than the OP of other regional playas. Our findings also indicated that the OP of the GSL dust was associated with metals, including Cu, Mn, Fe, and Al. This is the first study evaluating the oxidative potential of dust from the GSL, which improves our understanding of how increasing aridity, particularly desiccation of saline lakes, affects air quality and public health.

1. Introduction

The global increase in arid and semi-arid lands due to climate change (Huang et al., 2016; Song et al., 2018) has led to increased ambient dust levels and dust events (Achakulwisut et al., 2018; Schweitzer et al., 2018). Dust events negatively influence air quality and human health (Chen et al., 2021; De Longueville et al., 2010); such dust events occur when wind speeds surpass the threshold required for particles to be lifted from the soil (Jayaratne et al., 2011; Lei and Wang, 2014). Dust storms can transport harmful metals and metalloids, such as arsenic and lead, over long distances from the source region (Goudie, 2014; Morman and Plumlee, 2013). Previous studies have associated human exposure to dust events with adverse health effects, including lung cancer and cardiovascular mortality (Anderson et al., 2012; de Longueville et al., 2013; Zhang et al., 2016).

Increasing dust storms are a concern in the Salt Lake Valley due to the shrinking of the Great Salt Lake (GSL). GSL, which lies to the west of Utah's densely populated Wasatch Front (2.6 million people) (Nehra and Caplan, 2022), reached a historic low-level of 1275 m in 2022, with an exposed lakebed of over 1945 km^2 (Lang et al., 2023; Wurtsbaugh and Sima, 2022). Dust from the GSL contains enhanced levels of heavy metals, such as, Sb, and Cu, at levels that exceed the Environmental

* Corresponding author.
E-mail address: reuben.attah@utah.edu (R. Attah).

https://doi.org/10.1016/j.atmosenv.2024.120728
Received 2 March 2024; Received in revised form 21 May 2024; Accepted 30 July 2024
Available online 8 August 2024

Protection Agency (EPA) regional screening levels (Perry et al., 2019; Putman et al., 2022). On average, four to five dust storms occur in northern Utah annually (Hahnenberger and Nicoll, 2012; James Steenburgh et al., 2012); such dust events transport metal-contaminated dust from the GSL and present a concern for the air quality and health in the adjacent urban areas. Despite these concerns, no study has examined the impacts of dust from the GSL on human health.

Epidemiological studies in Utah's Wasatch Front have established connections between exposure to particulate matter (PM) and the heightened occurrence of hospital admissions due to respiratory and cardiovascular diseases (Brook et al., 2010; Horne et al., 2018; Leiser et al., 2019; Pope et al., 2008). Toxicological studies have also linked airborne dust exposure to adverse biological effects (Atafar et al., 2019; Courter et al., 2007; Faraji et al., 2018). However, the mechanisms for dust-related health and biological effects are not completely understood, although several studies have suggested that these effects could be related to dust's oxidative potential (Chirizzi et al., 2017; Lovett et al., 2018; Pant et al., 2015).

Oxidative potential (OP) measures the capacity of PM to generate reactive oxygen species (ROS) (Borlaza et al., 2018a; Yadav and Phuleria, 2020). The OP of PM has been reported as a more relevant metric to screen for biological effects than PM mass because several biologically significant properties such as size, composition, surface area, and bioaccessibility contribute to the OP of PM (Gao et al., 2020b; Janssen et al., 2014; Yang et al., 2015). Studies have associated ROS formation as a possible pathway linking dust exposure and adverse health effects, such as lung cancer and asthma (Li et al., 2003; Rogers and Cismowski, 2018). ROS are radicals or molecules with a single unpaired electron in their outermost shell of electrons (Bayir, 2005; Halliwell, 1992); the presence of unpaired electrons results in the high reactivity of ROS. Oxidative stress occurs when the generation of ROS exceeds the available human antioxidant defenses, which can lead to inflammation and damage to lipids, proteins, and DNA structures (Khansari et al., 2009; Schieber and Chandel, 2014; Sosa et al., 2013). Previous studies on PM-associated adverse health effects in Utah were focused on anthropogenic PM sources like transportation and industrial emissions (Ghio, 2004; Ou et al., 2020; Yu et al., 2023). Information regarding the OP of natural PM sources remains limited, and there is currently no available data regarding the OP of dust from the GSL. This study aims to fill this gap by evaluating the OP of GSL dust and comparing these to dust from regional playas.

The two widely used acellular assays to measure OP are the dithiothreitol (DTT) assay (Cho et al., 2005) and the ascorbic acid (AA) assay (Mudway et al., 2005) because they are cost-effective, have high reproducibility, and are a good indicator of adverse biological effects (Bates et al., 2019; Jiang et al., 2019; Ma et al., 2021). Assessing OP by DTT (OP^{DTT}) or AA (OP^{AA}) is based on the ability of redox-active components in PM to oxidize DTT (a surrogate for cellular antioxidants) or ascorbic acid (the most abundant antioxidant in lung fluids), respectively, by catalyzing the transfer of electrons from DTT or AA to molecular oxygen thereby promoting the formation of ROS (Fang et al., 2017a; Gao et al., 2020a).

Redox-active metals in dust particles have been linked to ROS formation and activating antioxidant-signaling pathways (Pardo et al., 2017; Rodríguez-Cotto et al., 2015). Water-soluble transition metals, such as Fe and Cu, participate in redox-cycling reactions, which may enhance DNA damage (Stohs, 1995; Valavanidis et al., 2005; Valko et al., 2005). Several studies have reported correlations between metals in urban dust (e.g., Ni, Cu, Cr, M, Cu, and As) with high OP^{DTT} and OP^{AA} (Chirizzi et al., 2017; Kajino et al., 2021; Nishita-Hara et al., 2019; Pant et al., 2015). Nishita-Hara et al. (2019) observed an increase in the particle-bound OP^{DTT} in PM_{10} (aerodynamic diameter less than 10 μm) dust samples from western Japan strongly correlated with the mineral dust-derived elements (Cu Al, Fe, Mn, Mg), suggesting that the concentration of mineral dust elements is an important controlling factor for the OP of coarse particles. Borlaza et al. (2018) revealed that OP activities of PM_{10} sampled from Korean sites increased during the spring and summer, possibly due to increased metals (Al, Fe, Mn, V, and Zn) caused by dust events. Mallone et al. (2011) also reported epidemiological evidence linking PM_{10} to elevated mortality rates during dust storm events in Italy; they attributed these findings to heightened exposure to metals in dust transported from the Sahara.

This study aims to (1) investigate the OP of 10 p.m.$_{10}$ dust samples (5 GSL, 4 from other regional playas, and reference Arizona test dust) using the DTT and AA assays and (2) compare the two OP methods (OP^{DTT} and OP^{AA}) to evaluate the sensitivity of the two OP methods to individual elements in the dust samples, (3) characterize the composition and bioaccessibility of the dust, and (4) correlate the OP and composition to identify components and sources contributing to the OP.

2. Methodology

2.1. Dust sample collection and preparation

Dust samples were collected from the exposed lakebed of the GSL and other regional playas (Sevier Dry Lake (SD), Tule Dry Lake dust (TD), Fish Springs Lake (FD), and West Desert (WD)) as shown in Fig. 1. Perry et al. (2019) performed a comprehensive examination of the GSL's exposed lakebed using an incremental sampling methodology (ISM). In accordance with ISM guidelines, they subdivided the lakebed into 10 Decision Units (DUs), each consisting of 122 subunits (SUs), as shown in Fig. 2. The longitude and latitude of the sample locations are also shown in Fig. 1. These samples were dried in an oven at a temperature of 105 °C for 24 h, followed by disaggregation and sieving to obtain dust samples with particle sizes less than 74 μm. Details on the site sampling procedure, preparation, and separation are provided in Perry et al. (2019). Arizona Test Dust (AD), a commonly used surrogate of atmospheric mineral dust for toxicology studies (Cote et al., 2018; Ichinose et al., 2008; Nishita-Hara et al., 2023), was used as reference dust.

It is essential to evaluate OP and bioaccessibility with inhalable PM, specifically PM_{10}; therefore, a system was developed to further separate PM_{10} samples from the coarse dust samples (<74 μm), as shown in Fig. 3. The coarse dust samples were placed into a flask and aerosolized using compressed air. The flask was placed on a magnetic stirrer to enhance the fluidization of the particles. The coarse dust samples passed through a MiniVol™ Tactical Air Sampler (Airmetrics USA), which contained a PM_{10} inlet separator and impactor to separate PM_{10} size fractions. The PM_{10} dust sample was collected on a 0.5 μm, 47 mm PTFE filter (Whatman, USA) at a flow rate of 5 LPM. This study characterized the composition and OP of the dust samples, and for the GSL, we selected five GSL dust samples (DU2-SU7, DU5-SU3, DU5-SU-4, DU5-SU10, DU9-SU14) to represent the range of the GSL samples. In total, we used 10 dust samples (5 GSL, 4 regional playas, and reference AD) for compositional and OP analysis.

2.2. Elemental composition analysis

Dust samples were treated using four different leaching solutions: phosphate buffer solution (PBS), Gamble's solution synthetic lung fluid (SLF), 1 M ammonium acetate buffer at pH = 7.0, and 1 M acetic acid. PBS was obtained from Sigma-Aldrich and treated with Chelex. SLF was obtained from Biochemazone and kept frozen until use; Ammonium acetate buffer and acetic acid solutions were prepared from concentrated ammonium and glacial acetic acid, both trace metal grade. The leaching treatment was done in parallel; each dust sample was split into four sub-samples, mixed with each leaching solution, and analyzed in the following way. Approximately 10 mg of dust for each sample/leaching solution was weighed in a 1.5 mL acid-leached polypropylene centrifuge tube, and 0.5 mL of each leaching solution was added and weighed. The vials were vortexed and then kept on a shaking table for 24 h at room temperature. The vials were then vortexed again and centrifuged at 10,000 rpm for 5 min. The clear supernatant leachates

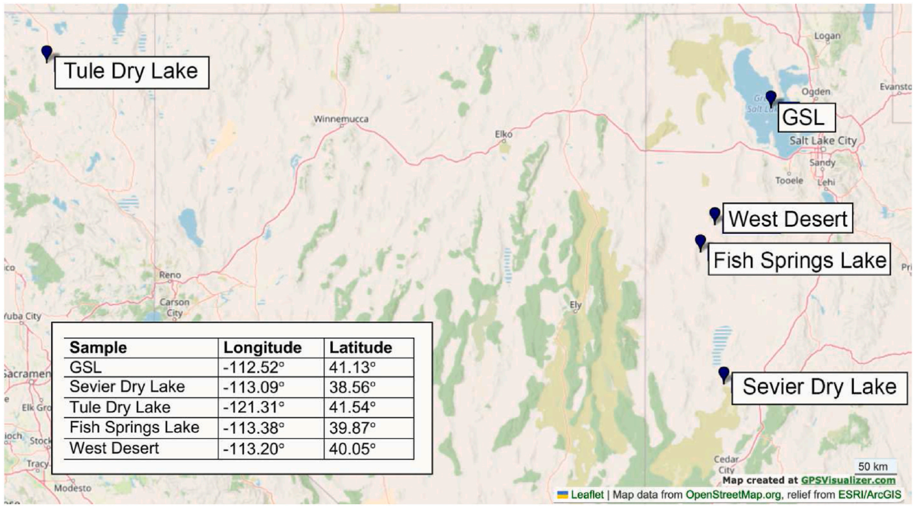

Sample	Longitude	Latitude
GSL	-112.52°	41.13°
Sevier Dry Lake	-113.09°	38.56°
Tule Dry Lake	-121.31°	41.54°
Fish Springs Lake	-113.38°	39.87°
West Desert	-113.20°	40.05°

Fig. 1. Map showing the location of sample sources.

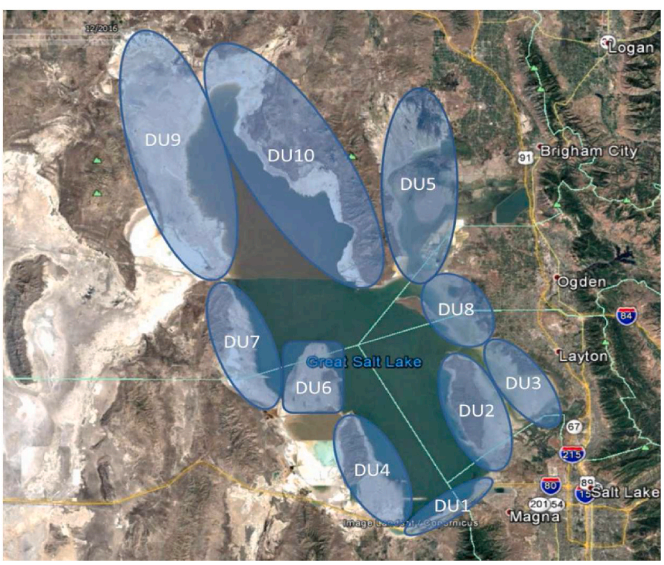

Fig. 2. Map showing the decision units (DUs) along the Great Salt Lake (Perry et al. (2019)).

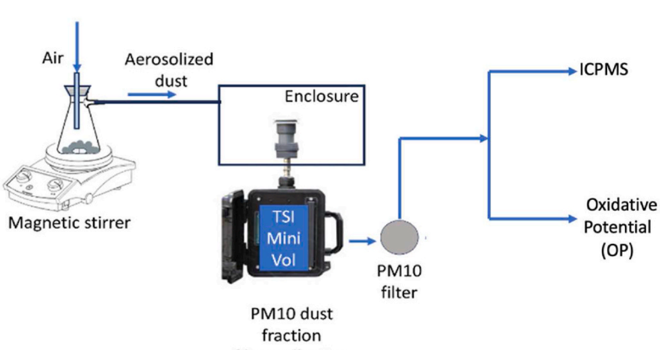

Fig. 3. Experimental setup to separate PM_{10} from the PM_{74} size fractionated dust samples.

were then diluted as follows: an aliquot of 0.100 mL of leachate was transferred into a polystyrene 14 mL tube, then acidified with 0.250 mL of concentrated HNO_3 (trace metal grade) and diluted with Type I water (IQ 7000, MilliporeSigma, Burlington, MA, US) to 10.0 mL. In this way, the total dilution factor was 5000. Elemental quantification was performed with a triple quadrupole inductively coupled plasma mass spectrometer (ICP-MS, Agilent 8900, Santa Clara, California). An external calibration curve was prepared from 1000 mg/L single element standards (Inorganic Ventures, Christiansburg, VA. Elements determined were Li, Be, Na, Mg, Al, K, Ca, Sc, Cr, Mn, Co, Ni, Cu, Ti, Zn, V, Fe, Ga, Rb, Sr, Y, As, Mo, Ag, Cd, Sb, Cs, Ba, La, Ce, Pr, Nd, Sm, Eu, Gd, Tb, Dy, Ho, Er, Yb, Lu, Tl, Pb, Bi, W, Th and U. Samples, calibration solutions, and blanks were added 10 ng/mL indium as internal standard and run in the ICP-MS using a dual-pass quartz spray chamber, PTFE nebulizer, dual-syringe introduction system (Teledyne, AVX 71000), platinum cones and sapphire injector in a platinum-shielded quartz torch. The limits of determination (LoD) were calculated as three times the standard deviation of the blanks, multiplied by the total dilution factor used for each sample. The instrument is in a filtered air positive pressure lab, and sample handling and dilutions were performed in laminar flow benches using calibrated pipettors (Eppendorf Reference, Hamburg, Germany). Data quality for both ICPMS quantification was determined by using Certified reference materials 1643f (Trace elements in water, National Institute of Standards and Technology, Gaithersburg, MD, with measured values within 5% of the certified values.

2.3. Oxidative potential analysis

The OP of the PM_{10} dust samples was assessed by both DTT and AA acellular assays. We also evaluated the effect of the extraction solvent on the OP of the dust samples by extracting the dust samples in two different aqueous solvents: phosphate buffered saline (PBS, pH = 7.4) and Gamble's solution (Biochemazone, pH = 7.4), which is a simulated lung fluid (SLF) solution used for accessing the bioaccessibility of PM in physiological fluids (Calas et al., 2017; Julien et al., 2011; Pietrogrande et al., 2021). The PBS was treated with Chelex® 100 resin (sodium form, BioRad, USA) to remove any trace metal ions that may catalyze oxidative reactions and to reduce background oxidation of DTT and AA.

Sample preparation: The PM_{10} particles were carefully scraped from the filter, weighed, and suspended in a glass vial using the two solvents. The suspensions were sonicated in an ultrasonic bath sonicator (Branson 2800, USA) for 15 min. A total of 1 mg/mL of the suspended dust PM_{10} sample solution was diluted to 100 μg/mL in PBS and SLF. The dust suspension was not filtered to include both soluble and insoluble species that may contribute to the total OP of the dust particles. Such a method has been used to study the OP of both soluble and insoluble species components of PM in physiological conditions (Borlaza et al., 2021; Daellenbach et al., 2020; Fang et al., 2017b; Gao et al., 2017).

Reagent preparation: Solutions of DTT and 5,5′-dithiobis-(2-nitrobenzoic acid) (DTNB) (Sigma-Aldrich, USA) were prepared in PBS at a concentration of 0.75 mM and 1 mM, respectively. Solution of AA (A92902 Sigma Aldrich, USA) was also prepared in PBS at the same concentration as DTT (i.e., 0.75 mM). The reagent solutions are sensitive to light. As a result, they were stored in vials wrapped in aluminum foil and kept in a dark environment throughout the experiment. A 35 μg/mL H_2O_2 and just PBS were used as positive and negative controls (referred to as blank), respectively.

DTT assay: 100 μL of the 0.75 mM DTT solution was added to 500 μL of 100 μg/mL of the dust samples (suspended in PBS (OP^{DTT} PBS) and SLF (OP^{DTT} SLF)), negative and positive control in different 1.5 mL vials at defined time points (0, 10, 20, 30, and 40 min). The mixture was vortexed and placed in an incubator (VWR, USA) under controlled conditions of 37 $^{\circ}C$ and pH of 7.4. At the end of the final time point of 40 min, the reaction vials were spun at 1.2k xg for 3 min using a microcentrifuge (AccuSpin Micro 17R, Fisher Scientific USA) to remove particles that might interfere with the absorbance reading. A 100 μL aliquot of the spun solution was transferred to a 96-well plate (Greiner Bio-One UV-Star Polystyrene) in triplicate, after which 50 μL of 1 mM DTNB solution was added to each aliquot. The negative control (blank) and positive control were run in duplicates. The unconsumed DTT reacts with DTNB to form a colored product, 2-nitro 5-thiobenzoic acid (TNB); the absorbance of the TNB was measured at a wavelength of 412 nm, using a plate reader (Molecular Devices, CA, USA).

AA assay: 25 μl of AA solution was added to 100 μg/mL of the dust samples (suspended in PBS (OP^{AA} PBS) and SLF (OP^{AA} SLF)) in a 96-well plate (Greiner Bio-One UV-Star COC). The rate of AA consumption was directly measured in the plate reader at 265 nm at a time interval of 10 min for 2 h. The 96-well plate was auto-shaken for 60 s before each absorbance reading, and all the sample absorbance measurements were done in triplicate. The absorbance from the dust samples without any AA was also measured and subtracted from the final sample absorbance readings to remove the contribution of the background particle absorbance.

The sample's DTT or AA consumption rate (n_s, pmol/min) was determined from the linear slope and intercept of measured absorbance versus time. We limited DTT and AA consumption to less than 20% of the initial concentration to achieve a linear consumption rate. The consumption rate (n_s) is given by:

$$n_s = -\sigma_{abs} \times \frac{N_0}{Abs_0}$$

Where , σ_{abs} is the slope of absorbance versus time, N_0 is the initial amount of DTT or AA in pmol, and Abs_0 is the initial absorbance calculated from the intercept of linear regression of absorbance versus time.

OP of the sample (pmol/min/μg) is defined by the DTT or AA consumption rate normalized by sample mass added to the reaction mixture. This is given by:

$$OP_{sample} = \frac{n_s - n_{blank}}{m_{sample}}$$

Where n_{blank} *is* the rate of DTT or AA consumption in the blank, and m_{sample} is the mass of the sample in the reaction mixture.

2.4. Data analysis

We used a one-way analysis of variance (ANOVA, astatsa.com online) to assess differences in OP among the ten samples. Subsequently, we conducted a post-hoc Tukey HSD test to identify OP differences between dust sample pairs (PBS and SLF). The results are displayed as the standard deviation of the mean. Significance levels of $p < 0.01$ and $p < 0.05$ were used to determine statistical significance. We also conducted a Pearson correlation analysis to assess the relationships between OP responses in various OP assays (OP^{DTT} and OP^{AA}) and the correlation between different extraction solvents (PBS and SLF). Additionally, we used principal component analysis to investigate the association between OP responses and metal concentrations in the dust samples.

3. Results and discussion

3.1. Elemental concentrations of dust samples

Table 1 shows the elemental concentrations in SLF-extracted dust samples. The SLF-extracted elemental concentration enables investigation of the bioaccessibility and fate of deposited dust particles in lung fluid. Table S1 (Supplementary material) contains a more comprehensive list of the mass composition of the dust samples as measured by ICPMS. The United States EPA developed regional screening levels (RSLs) as a reference for evaluating the ecological risk associated with soil contaminants. The first step in our analysis involved comparing our dust composition measurements against these RSLs. We removed all elements (Be, Co, Ni, Se, Cd, La, Ce, Pr, Nd, Sm, Eu, Gd, Tb, Dy, Ho, Er, Yb, Lu, Th) that had mass concentration values below their minimum detection limit (MDL). Out of the 24 remaining elements, 8 were not found in the EPA RSL database, suggesting that there is insufficient information to assess health concerns linked to these elements. These 8 elements include Na, Mg, Ca, K, Rb, Y, Cs, and S.

The metal concentrations, shown in Table 1, indicate a high concentration of crustal elements (Na, Mg, K, Ca, and S). These crustal elements are associated with evaporated minerals that form on the surface of the lakebed (Alkhayer et al., 2023; Cabestrero et al., 2018; Levy et al., 1999). Various transition metals were detected in all the samples. The average concentration of transition metals (B, Mn, Fe, Cu, V) and metalloids (Li, Rb, As, Sb, Cs, Pb) from the GSL sites were higher than those in other regional playas. Arsenic is of particular focus at the GSL due to reports of its enhanced concentrations in dust aerosols and its known toxicity (Baxter and Butlerreditors., 2020; Castro-Severyn et al., 2020; Wurtsbaugh, 2012). Among the trace elements measured, lithium and arsenic concentrations exceeded the soil residential RSL in most of the GSL sites and other regional playas collected in this study, as shown in Fig. 4. Previous studies have also reported the enrichments of trace elements such as arsenic and lead at dust collection sites within the GSL and Wasatch front (Goodman et al., 2019; Putman et al., 2022; Reynolds et al., 2010; Thorsen et al., 2017).

3.2. OP using AA and DTT assays

Fig. 5 shows the OP^{AA} of all the dust samples from different sampling sites in PBS and SLF normalized by the sample mass. The OP^{AA}PBS and OP^{AA}SLF of GSL dust samples were generally higher compared to other regional dust playas, including the reference AD. Notably, the OP^{AA}PBS of the DU5-SU4 GSL dust sample was significantly higher than the OP^{AA}PBS of the AD and other regional playas ($p < 0.05$). The mean OP^{AA} PBS and OP^{AA} SLF of GSL samples were within the ranges of 3 ± 0.03 to 5.57 ± 0.14 pmol/min/μg and 1.95 ± 0.05 to 2.98 ± 0.14 pmol/min/μg) respectively.

Fig. 6 shows higher OP^{DTT} of all the dust samples from different sampling sites in PBS and SLF normalized by the sample mass. The OP^{DTT}PBS and OP^{DTT}SLF of most of the GSL dust samples were also higher compared to other regional dust playas but lower than the OP^{DTT} of reference AD. Specifically, the OP^{DTT}PBS and OP^{DTT}SLF of the DU5-SU4 GSL sample were significantly higher than the OP^{DTT} of other regional playas for both solvents. Overall, the OP^{DTT} PBS and OP^{DTT} SLF of GSL samples were within the ranges of 1.75 ± 0.24 to 4.89 ± 0.5 pmol/min/μg and 1.15 ± 0.02 to 3.85 ± 0.07 pmol/min/μg, respectively.

Several studies have reported adverse biological outcomes from exposure to AD (Cote et al., 2018; Ichinose et al., 2008; Kameda et al.,

Table 1
Concentrations of selected elements (mg of element per kg of sample; mg/kg) in SLF leachate measured by ICPMS.

Sample	AD	WD	TD	SD	FD	DU2-SU7	DU5-SU3	DU5-SU4	DU5-SU10	DU9-SU14
Li	3.32	16.5	8.05	6.83	22	19.3	9.41	20.1	7.25	17.9
B	1	26.1	26.4	46.3	109	111	46.4	33.6	19.2	26.5
Na	22,001	32,806	27,308	33,149	34,454	41,974	47,375	35,468	44,188	38,838
Mg	282	1901	671	1610	2529	7386	2671	4859	1263	1315
Al	7.33	1	1	2.38	1.5	1	1.5	1.34	1.55	5.36
K	683	1924	3066	1934	2139	2928	3076	3685	1583	3132
Ca	717	1535	1556	3015	11162	3628	1649	1907	481	1956
Mn	1.61	0.66	0.28	0.15	0.60	1.12	0.42	1.75	0.80	1.69
Fe	25.4	39.6	6.97	8.59	14.2	9.26	11.68	84.2	3.32	19.8
Cu	0.05	0.14	<MDL	<MDL	<MDL	0.08	<MDL	0.45	<MDL	<MDL
V	1	0.52	0.84	0.43	0.28	0.22	0.28	0.55	0.63	1.15
Cr	0.43	0.80	0.13	0.18	0.23	0.14	0.17	1.36	0.05	0.29
Rb	0.89	2.88	4.35	1.17	9.07	7.76	9.27	7.73	2.91	6.50
Sr	27	155	138	84	340	151	81	46	63	77
Y	0.004	0.003	0.002	0.003	0.005	0.006	0.006	0.008	0.002	0.010
As	0.34	1.04	4.61	1.13	1.52	2.64	1.98	1.00	1.61	1.63
Mo	0.08	0.59	6.74	1.19	0.62	3.64	0.38	0.65	0.19	0.85
Sb	0.06	0.04	0.03	0.04	0.02	0.22	0.08	0.06	0.02	0.04
Cs	0.01	0.01	0.06	0.01	0.05	0.09	0.05	0.03	0.01	0.09
Ba	13.6	21.5	10.2	3.8	4.25	3.83	3.68	7.02	0.07	7.71
Tl	0.01	0.00	0.02	0.00	0.01	0.02	0.01	0.02	0.00	0.01
Pb	0.02	0.01	<MDL	<MDL	<MDL	0.05	0.03	0.03	0.00	0.04
U	0.12	1.84	2.28	1.37	2.31	1.90	1.21	0.69	0.81	0.67
S	132	6611	5056	9805	24,168	24,959	6961	7704	2086	2670

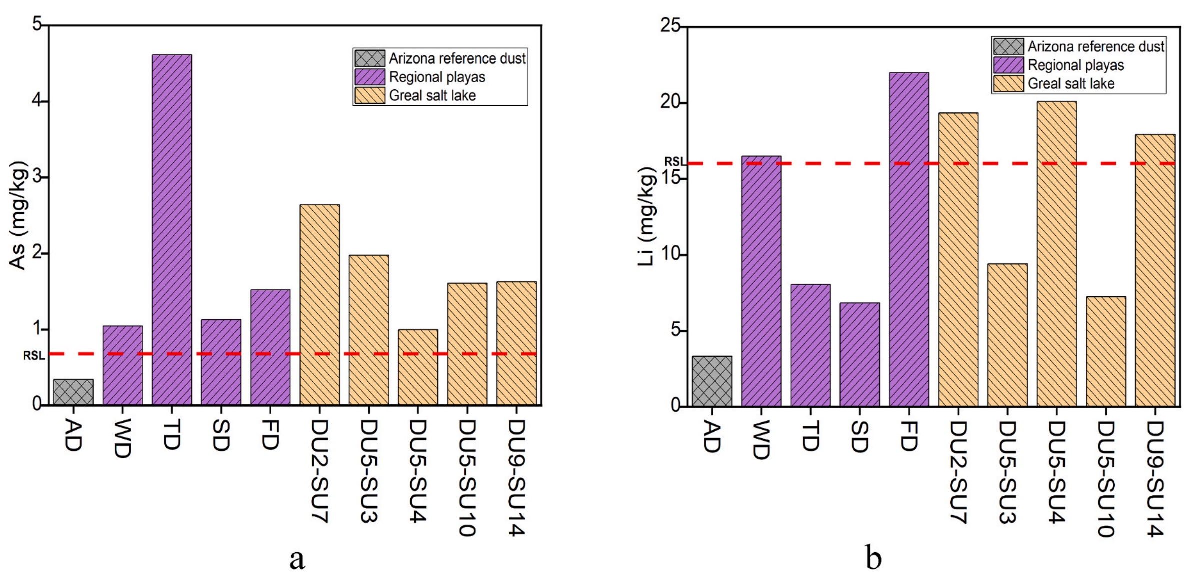

Fig. 4. Elemental mass concentrations (mg/kg) for (a) arsenic and (b) lithium compared with EPA-recommended soil residential screening levels determined by ICP-MS analysis in SLF extract. The red dashed horizontal line indicates the regional screening level for each element.

2016; Nishita-Hara et al., 2023). Ichinose et al. reported that AD caused a slight increase of neutrophils in bronchoalveolar lavage fluids and pro-inflammatory mediators, such as keratinocyte chemoattractant masters of the air. By comparing the OP of GSL and other regional playas to AD, we can assess the relative health risks associated with dust exposure from the GSL.

The OP^{AA} of some of the GSL samples, particularly DU5-SU4, were generally higher compared to AD samples and other regional playas. This suggests that the GSL contains more redox-active species than AD and other playas. In general, the measured OP^{DTT} of GSL samples in this study is within the range of previously reported OP values (3–10 pmol/min/μg) from dust sources in Saudi Arabia (Altuwayjiri et al., 2022), a coastal site on the Central Mediterranean Sea (Perrone et al., 2019), and the Sahara (Chirizzi et al., 2017), but considerably lower than those reported for mineral soil dust in Japan (23 pmol/min/μg) (Nishita-Hara et al., 2023). The differences in OP between the sites may be partially attributed to varying concentrations of redox-active species. As seen in Table 1, the concentrations of redox-active metals such as Mn, Fe, and Cu in the GSL dust samples were higher compared to the concentrations in other regional playas. Several studies have reported that transition metals may play a role in triggering oxidative stress and inflammation in the lungs by catalyzing the formation of ROS through participation in Fenton reactions and generating highly reactive superoxide radicals (Jomova et al., 2023; Jomova and Valko, 2011; Kim et al., 2021; Valko et al., 2016).

3.3. Relationship between OP and elemental composition

To gain a deeper insight into the primary chemical constituents associated with the higher OP of the dust samples, the relationship between OP values and metal components in the dust samples was assessed using Pearson's r correlation coefficients. Figs. 7 and 8 show the

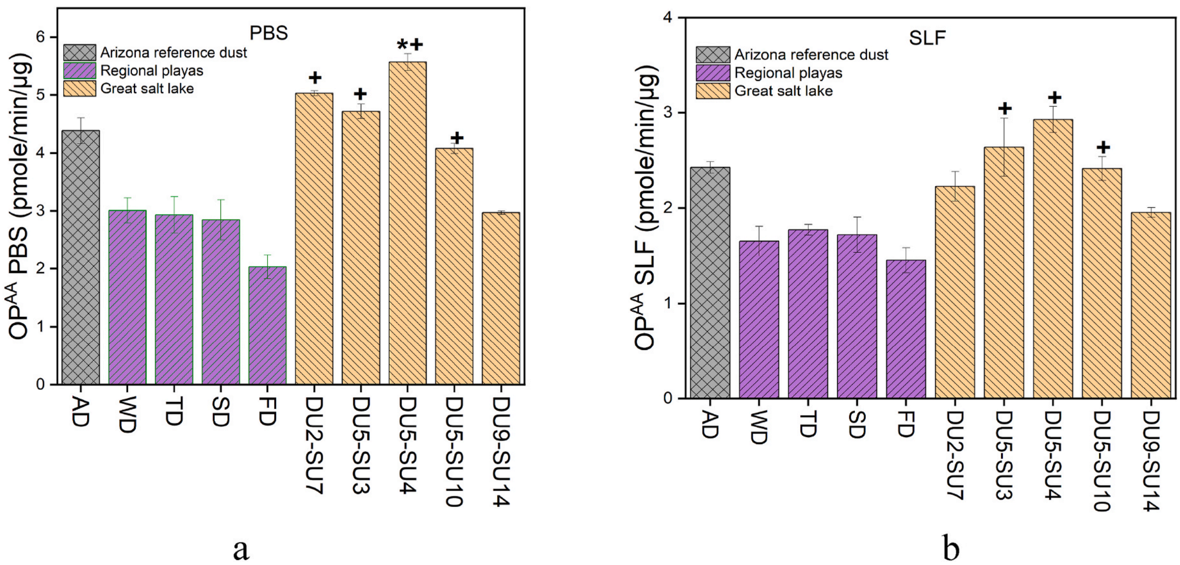

Fig. 5. OP^{AA} of the dust samples in (a) PBS and (b) SLF. Error bars represent the standard deviation of the mean from three replicate measurements. Asterisks denote significantly higher than AD (*$p < 0.05$), and plus signs denote significantly higher than other regional playas (+$p < 0.05$).

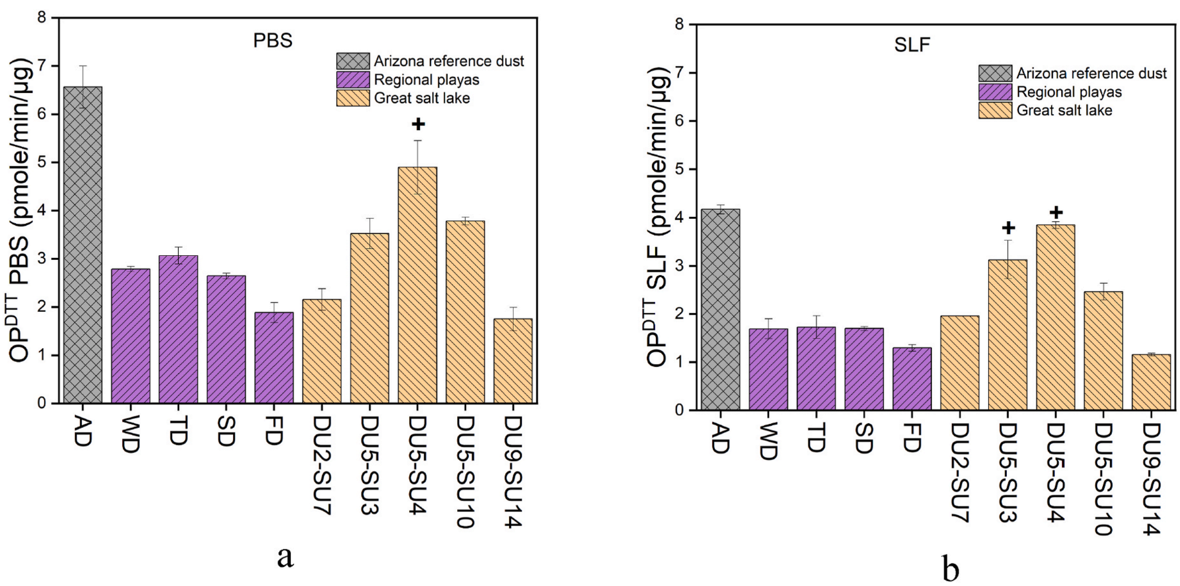

Fig. 6. OP^{DTT} of the dust samples at different sampling sites in (a) PBS and (b) SLF. Error bars represent the standard deviation of the mean from three replicate measurements, and plus signs denote Significantly higher than other regional playas (+$p < 0.05$).

correlation coefficients between OP values and elemental concentration.

In the AA assay (Fig. 7), we observed a positive correlation between the OP^{AA} and metal concentrations for the following constituents: (OP^{AA}PBS: Pb, $r = 0.64$; Cu, $r = 0.61$; Mn, $r = 0.49$; Fe, $r = 0.43$; and Cr, $r = 0.38$) and (OP^{AA}SLF: Pb, $r = 0.53$; Mn, $r = 0.52$; Cu, $r = 0.5$; Fe, $r = 0.47$; and Cr, $r = 0.4$). For the DTT assay (Fig. 8), the correlation coefficients between the OP (OP^{DTT}-PBS and OP^{DTT}-SLF) and metal concentrations were positive for (OP^{DDT}PBS: Al, $r = 0.46$; Mn, $r = 0.4$; Fe, $r = 0.4$; Cu, $r = 0.39$; and Cr, $r = 0.39$) and (OP^{DTT}SLF: Fe, $r = 0.48$; Cu, $r = 0.45$; Cr, $r = 0.45$; Mn, $r = 0.44$; and Al, $r = 0.31$). These results suggest an association between the redox activity of these metals in the dust samples to generate ROS. Previous studies on the OP of PM_{10} have linked AA and DTT to redox-active transition metals, especially Cu and Mn (Malakootian et al., 2022; Pietrogrande et al., 2018). The relationship between OP values and metal components in the dust samples was also assessed using principal component analysis (PCA) factors. The first two principal components combined explained about 55–57 % of the total variance in the data set in the OP^{AA} and OP^{DTT} assays, respectively. Fig. S2 shows the relationship between metal composition and OP in the OP^{AA}-PBS assay. The component space (Fig. S2) indicates that PC1 accounts for 34% of the total variability in the dataset. PC2 follows PC1, explaining approximately 23% of the total variance. Notably, Fe, Cu, Cr, Mn, and Pb are clustered in the same quadrant as the OP, indicating their correlation and relative distance to the OP variable compared to other elemental metals. This correlation pattern extends similarly across other assays (Figs. S2–S5), as shown in the supplementary material.

3.4. *Effect of assay and solvent choice on OP*

Figs. 9 and 10 show the correlation between OP values for the two OP assays (AA and DTT) and two solvents (PBS and SLF). The OP assays (AA and DTT) display different sensitivity toward redox-active species in the dust samples (Fig. 9). The correlation between OP^{AA} PBS and OP^{DTT} PBS was 0.56, and the correlation between OP^{AA} SLF and OP^{DTT} SLF was

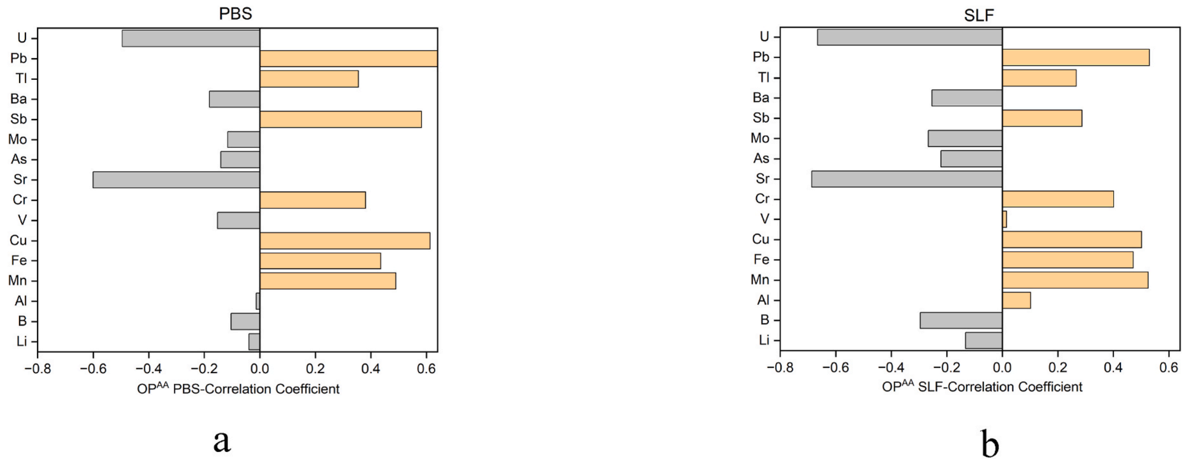

Fig. 7. Bar chart of the correlation coefficients between the OP^{AA} (OP^{AA} dust samples suspended in (a) PBS and (b) SLF) and metal concentration of all dust samples (GSL, regional playas, and AD).

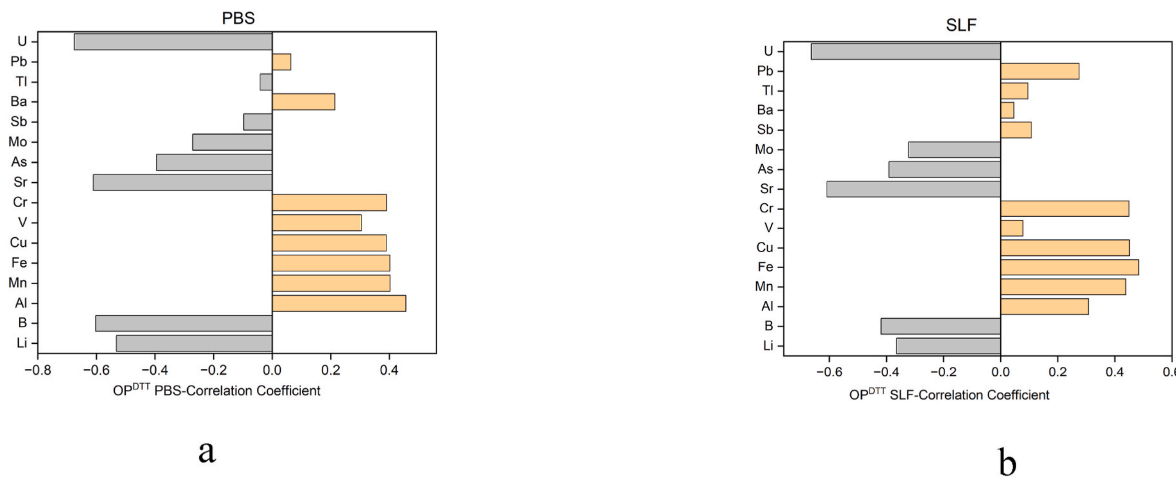

Fig. 8. Bar chart of the correlation coefficient between the OP^{DTT} (OP^{DTT} dust samples suspended in (a) PBS and (b) SLF) and metal concentration of all dust samples (GSL, regional playas, and AD).

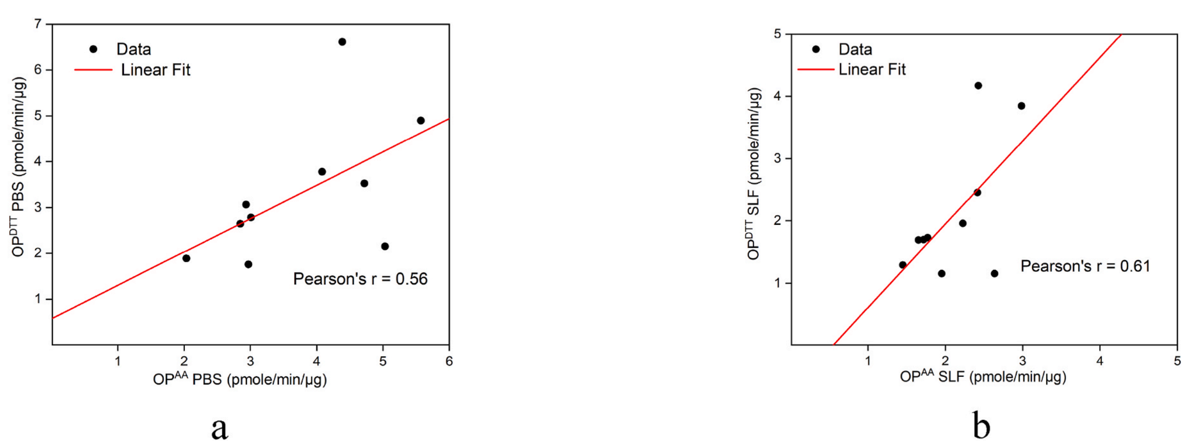

Fig. 9. Correlation between OP assays for all the dust samples (GSL, regional playas, and AD).

0.61. This indicates that the two OP assays (AA and DTT) display different sensitivity toward redox-active species in the dust samples suspended in the solvent. Figs. 5 and 6 show that the OP^{AA} for each sample was higher than the corresponding OP^{DTT} for each solvent except for the AD sample, most likely because the AA assay was more sensitive to redox-active metals in the dust samples. The OP^{AA} assay displayed sensitivity towards Pb, Cu, and Mn in both solvents, while the OP^{DTT} was associated with Al and Fe. OP assays exhibit distinct responses to redox-active compounds due to the unique reaction mechanisms underlying each assay (Bates et al., 2019; Clemente et al., 2023; Visentin et al.,

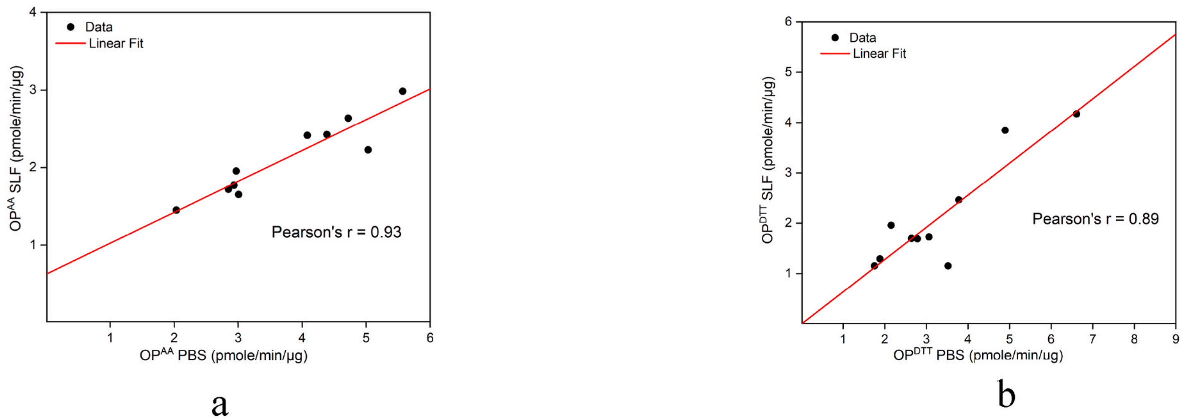

Fig. 10. Correlation between OP solvents for all the dust samples (GSL, regional playas, and AD).

2016a). The findings align with some previous studies (Bates et al., 2019; Clemente et al., 2023; Perrone et al., 2019; Shahpoury et al., 2022) but contradict others that have observed similar sensitivity of both assays to the same redox-active species (Pietrogrande et al., 2019; Visentin et al., 2016b). Although there is no consensus on the most appropriate assay for accessing the OP of PM (Ayres et al., 2008; Calas et al., 2018; Sauvain et al., 2013), comparing different acellular OP measurements for a given set of ambient PM samples is important because the assays could potentially provide complementary information on the OP of the PM. This information can also give insight into the chemical composition responsible for the assay responses, facilitating further research into health effects and the development of more effective control strategies.

Similar to the choice of assay, the values of OP also differ based on the choice of solvent (Fig. 10). Although the two solvents exhibited similar trends in both OP assays (OP^{AA} $r = 0.93$ and OP^{DTT} $r = 0.89$), overall, the OP-PBS of most of the dust samples were significantly higher than the OP-SLF ($P < 0.05$) for both OP assays (Fig. S1). Such differences may be mainly ascribed to variations in soluble fractions of redox-active species in the two solvents. Our findings are consistent with several literature papers that reported high redox activity in PBS compared to SLF (Cigánková et al., 2021; Expósito et al., 2023; Pietrogrande et al., 2021). Pietrogrande et al. observed that the OP^{AA}PBS was nearly double that of OP^{AA}SLF and methanol extracts. Aside from the differences in solubility, the reduction of OP in SLF compared to PBS may also be explained by the formation of metal complexes in SLF that decrease antioxidant oxidation. Previous studies have suggested that chloride compounds play a role in reducing the redox activity of metals in AA solution (Cigánková et al., 2021; Expósito et al., 2023; Murekhina et al., 2022). Murekhina et al. (2022) proposed that the reduction of AA oxidation in SLF was due to the formation of Cu (I) and Cu (II) complexes when chlorides in SLF react with Cu. These complexes exhibit distinct oxidation rates compared to the unbound cation.

4. Conclusions

The study investigated the OP (using the AA and DTT assays) and elemental composition of PM_{10} dust from the GSL, other regional playas, and a reference AD. Our results suggest that GSL dust PM_{10} generally exhibits greater OP than other regional playas, which is potentially concerning for the residents who live adjacent to the GSL lakebed. We also found that the concentration of As in all the GSL dust samples exceeded the EPA soil residential RSL, and the concentrations of Li in some of the GSL dust samples exceeded the EPA soil residential RSL. Our statistical analysis (PCA coupled with correlation analysis) indicated that metals such as Pb, Cu, Mn, Fe, Cr, and Al were associated with high OP of the GSL dust. This study showed that the choice of assay and extraction solvent affects the OP activity of redox-active fractions of PM_{10} and highlights the importance of using different OP assays to investigate the sensitivity of redox-active species towards antioxidant surrogates.

Funding

Support for this research was provided by a grant from the Wilkes Center for Climate Science and Policy incentive seed grant under grant no.2500-36306 and by the National Science Foundation under grant no. 2012091 (Collaborative Research Network Cluster: Dust in the Critical Zone) and under grant no. 2228600.

CRediT authorship contribution statement

Reuben Attah: Writing – review & editing, Writing – original draft, Methodology, Investigation, Formal analysis, Conceptualization. **Kamaljeet Kaur:** Writing – review & editing, Methodology, Investigation, Formal analysis. **Kevin D. Perry:** Writing – review & editing, Methodology, Investigation, Funding acquisition, Formal analysis, Conceptualization. **Diego P. Fernandez:** Writing – review & editing, Methodology, Investigation. **Kerry E. Kelly:** Writing – review & editing, Supervision, Methodology, Investigation, Funding acquisition, Formal analysis, Conceptualization.

Declaration of competing interest

The authors declare that they have no known competing financial interests or personal relationships that could have appeared to influence the work reported in this paper.

Data availability

Data will be made available on request.

Acknowledgments

We are grateful to Vishal Verma from the University of Illinois Urbana-Champaign for sharing his expertise on oxidative potential assay.

Appendix A. Supplementary data

Supplementary data to this article can be found online at https://doi.org/10.1016/j.atmosenv.2024.120728.

References

Achakulwisut, P., Mickley, L.J., Anenberg, S.C., 2018. Drought-sensitivity of fine dust in the US Southwest: implications for air quality and public health under future climate change. Environ. Res. Lett. 13 https://doi.org/10.1088/1748-9326/aabf20.

Alkhayer, M., Karimian Eghbal, M., Hamzehpour, N., rahnemaie, R., 2023. Brine geochemical changes and salt crust evolution of Lake Urmia in Iran. Catena 231. https://doi.org/10.1016/j.catena.2023.107310.

Anderson, J.O., Thundiyil, J.G., Stolbach, A., 2012. Clearing the air: a review of the effects of particulate matter air pollution on human health. J. Med. Toxicol. https://doi.org/10.1007/s13181-011-0203-1.

Atafar, Z., Pourpak, Z., Yunesian, M., Nicknam, M.H., Hassanvand, M.S., Soleimanifar, N., Saghafi, S., Alizadeh, Z., Rezaei, S., Ghanbarian, M., Ghozikali, M. G., Osornio-Vargas, A.R., Naddafi, K., 2019. Proinflammatory effects of dust storm and thermal inversion particulate matter (PM10) on human peripheral blood mononuclear cells (PBMCs) in vitro: a comparative approach and analysis. J Environ Health Sci Eng 17, 433–444. https://doi.org/10.1007/s40201-019-00362-1.

Ayres, J.G., Borm, P., Cassee, F.R., Castranova, V., Donaldson, K., Ghio, A., Harrison, R. M., Hider, R., Kelly, F., Kooter, I.M., Marano, F., Maynard, R.L., Mudway, I., Nel, A., Sioutas, C., Smith, S., Baeza-Squiban, A., Cho, A., Duggan, S., Froines, J., 2008. Evaluating the toxicity of airborne particulate matter and nanoparticles by measuring oxidative stress potential - a workshop report and consensus statement. In: Inhalation Toxicology, pp. 75–99. https://doi.org/10.1080/08958370701665517.

Bates, J.T., Fang, T., Verma, V., Zeng, L., Weber, R.J., Tolbert, P.E., Abrams, J.Y., Sarnat, S.E., Klein, M., Mulholland, J.A., Russell, A.G., 2019. Review of acellular assays of ambient particulate matter oxidative potential: methods and relationships with composition, sources, and health effects. Environ. Sci. Technol. 53, 4003–4019. https://doi.org/10.1021/acs.est.8b03430.

Baxter, B., Butlerreditors, J., 2020. Great Salt Lake Biology. Springer International Publishing, Cham. https://doi.org/10.1007/978-3-030-40352-2.

Bayir, H., 2005. Reactive oxygen species. Crit. Care Med. 33 https://doi.org/10.1097/01.CCM.0000186787.64500.12.

Borlaza, L.J.S., Cosep, E.M.R., Kim, S., Lee, K., Joo, H., Park, M., Bate, D., Cayetano, M. G., Park, K., 2018a. Oxidative potential of fine ambient particles in various environments. Environ. Pollut. 243, 1679–1688. https://doi.org/10.1016/j.envpol.2018.09.074.

Borlaza, L.J.S., Weber, S., Jaffrezo, J.L., Houdier, S., Slama, R., Rieux, C., Albinet, A., Micallef, S., Trébluchon, C., Uzu, G., 2021. Disparities in particulate matter (PM10) origins and oxidative potential at a city scale (Grenoble, France) - Part 2: sources of PM10 oxidative potential using multiple linear regression analysis and the predictive applicability of multilayer perceptron neural network analysis. Atmos. Chem. Phys. 21, 9719–9739. https://doi.org/10.5194/acp-21-9719-2021.

Brook, R.D., Rajagopalan, S., Pope, C.A., Brook, J.R., Bhatnagar, A., Diez-Roux, A.V., Holguin, F., Hong, Y., Luepker, R.V., Mittleman, M.A., Peters, A., Siscovick, D., Smith, S.C., Whitsel, L., Kaufman, J.D., 2010. Particulate matter air pollution and cardiovascular disease: an update to the scientific statement from the american heart association. Circulation. https://doi.org/10.1161/CIR.0b013e3181dbece1.

Cabestrero, Ó., del Buey, P., Sanz-Montero, M.E., 2018. Biosedimentary and geochemical constraints on the precipitation of mineral crusts in shallow sulphate lakes. Sediment. Geol. 366, 32–46. https://doi.org/10.1016/j.sedgeo.2018.01.005.

Calas, A., Uzu, G., Martins, J.M.F., Voisin, Di, Spadini, L., Lacroix, T., Jaffrezo, J.L., 2017. The importance of simulated lung fluid (SLF) extractions for a more relevant evaluation of the oxidative potential of particulate matter. Sci. Rep. 7 https://doi.org/10.1038/s41598-017-11979-3.

Calas, A., Uzu, G., Kelly, F.J., Houdier, S., Martins, J.M.F., Thomas, F., Molton, F., Charron, A., Dunster, C., Oliete, A., Jacob, V., Besombes, J.L., Chevrier, F., Jaffrezo, J.L., 2018. Comparison between five acellular oxidative potential measurement assays performed with detailed chemistry on PM10 samples from the city of Chamonix (France). Atmos. Chem. Phys. 18, 7863–7875. https://doi.org/10.5194/acp-18-7863-2018.

Castro-Severyn, J., Pardo-Esté, C., Mendez, K.N., Morales, N., Marquez, S.L., Molina, F., Remonsellez, F., Castro-Nallar, E., Saavedra, C.P., 2020. Genomic Variation and Arsenic Tolerance Emerged as Niche Specific Adaptations by Different Exiguobacterium Strains Isolated From the Extreme Salar de Huasco Environment in Chilean – Altiplano. Front. Microbiol. 11 https://doi.org/10.3389/fmicb.2020.01632.

Chen, C.Y., Chen, H.W., Sun, C.T., Chuang, Y.H., Nguyen, K.L.P., Lin, Y.T., 2021. Impact assessment of river dust on regional air quality through integrated remote sensing and air quality modeling. Sci. Total Environ. 755 https://doi.org/10.1016/j.scitotenv.2020.142621.

Chirizzi, D., Cesari, D., Guascito, M.R., Dinoi, A., Giotta, L., Donateo, A., Contini, D., 2017. Influence of Saharan dust outbreaks and carbon content on oxidative potential of water-soluble fractions of PM2.5 and PM10. Atmos. Environ. 163, 1–8. https://doi.org/10.1016/j.atmosenv.2017.05.021.

Cho, A.K., Sioutas, C., Miguel, A.H., Kumagai, Y., Schmitz, D.A., Singh, M., Eiguren-Fernandez, A., Froines, J.R., 2005. Redox activity of airborne particulate matter at different sites in the Los Angeles Basin. Environ. Res. 99, 40–47. https://doi.org/10.1016/j.envres.2005.01.003.

Cigánková, H., Mikuška, P., Hegrová, J., Krajčovič, J., 2021. Comparison of oxidative potential of PM1 and PM2.5 urban aerosol and bioaccessibility of associated elements in three simulated lung fluids. Sci. Total Environ. 800 https://doi.org/10.1016/j.scitotenv.2021.149502.

Clemente, Gil-Moltó, J., Yubero, E., Juárez, N., Nicolás, J.F., Crespo, J., Galindo, N., 2023. Sensitivity of PM10 oxidative potential to aerosol chemical composition at a Mediterranean urban site: ascorbic acid versus dithiothreitol measurements. Air Qual Atmos Health 16, 1165–1172. https://doi.org/10.1007/s11869-023-01332-1.

Cote, C.D., Schneider, S.R., Lyu, M., Gao, S., Gan, L., Holod, A.J., Chou, T.H.H., Styler, S. A., 2018. Photochemical production of singlet oxygen by urban road dust. Environ. Sci. Technol. Lett. 5, 92–97. https://doi.org/10.1021/acs.estlett.7b00533.

Courter, L.A., Musafia-Jeknic, T., Fischer, K., Bildfell, R., Giovanini, J., Pereira, C., Baird, W.M., 2007. Urban dust particulate matter alters PAH-induced carcinogenesis by inhibition of CYP1A1 and CYP1B1. Toxicol. Sci. 95, 63–73. https://doi.org/10.1093/toxsci/kfl137.

Daellenbach, K.R., Uzu, G., Jiang, J., Cassagnes, L.E., Leni, Z., Vlachou, A., Stefenelli, G., Canonaco, F., Weber, S., Segers, A., Kuenen, J.J.P., Schaap, M., Favez, O., Albinet, A., Aksoyoglu, S., Dommen, J., Baltensperger, U., Geiser, M., El Haddad, I., Jaffrezo, J.L., Prévôt, A.S.H., 2020. Sources of particulate-matter air pollution and its oxidative potential in Europe. Nature 587, 414–419. https://doi.org/10.1038/s41586-020-2902-8.

De Longueville, F., Hountondji, Y.C., Henry, S., Ozer, P., 2010. What do we know about effects of desert dust on air quality and human health in West Africa compared to other regions? Sci. Total Environ. https://doi.org/10.1016/j.scitotenv.2010.09.025.

De Longueville, F., Ozer, P., Doumbia, S., Henry, S., 2013. Desert dust impacts on human health: an alarming worldwide reality and a need for studies in West Africa. Int. J. Biometeorol. 57, 1–19. https://doi.org/10.1007/s00484-012-0541-y.

Expósito, A., Markiv, B., Santibáñez, M., Fadel, M., Ledoux, F., Courcot, D., Fernández-Olmo, I., 2023. Ascorbate oxidation driven by PM2.5-bound metal(loid)s extracted in an acidic simulated lung fluid in relation to their bioaccessibility. Air Qual Atmos Health. https://doi.org/10.1007/s11869-023-01436-8.

Fang, T., Guo, H., Zeng, L., Verma, V., Nenes, A., Weber, R.J., 2017a. Highly acidic ambient particles, soluble metals, and oxidative potential: a link between sulfate and aerosol toxicity. Environ. Sci. Technol. 51, 2611–2620. https://doi.org/10.1021/acs.est.6b06151.

Fang, T., Zeng, L., Gao, D., Verma, V., Stefaniak, A.B., Weber, R.J., 2017b. Ambient size distributions and lung deposition of aerosol dithiothreitol-measured oxidative potential: contrast between soluble and insoluble particles. Environ. Sci. Technol. 51, 6802–6811. https://doi.org/10.1021/acs.est.7b01536.

Faraji, M., Pourpak, Z., Naddafi, K., Nodehi, R.N., Nicknam, M.H., Shamsipour, M., Rezaei, S., Ghozikali, M.G., Ghanbarian, M., Mesdaghinia, A., 2018. Effects of airborne particulate matter (PM10) from dust storm and thermal inversion on global DNA methylation in human peripheral blood mononuclear cells (PBMCs) in vitro. Atmos. Environ. 195, 170–178. https://doi.org/10.1016/j.atmosenv.2018.09.042.

Gao, D., Fang, T., Verma, V., Zeng, L., Weber, R.J., 2017. A method for measuring total aerosol oxidative potential (OP) with the dithiothreitol (DTT) assay and comparisons between an urban and roadside site of water-soluble and total OP. Atmos. Meas. Tech. 10, 2821–2835. https://doi.org/10.5194/amt-10-2821-2017.

Gao, D., Godri Pollitt, K.J., Mulholland, J.A., Russell, A.G., Weber, R.J., 2020a. Oxidative potential assessed by two acellular assays. Atmos. Chem. Phys. 20, 5197–5210. https://doi.org/10.5194/acp-20-5197-2020.

Gao, D., Ripley, S., Weichenthal, S., Godri Pollitt, K.J., 2020b. Ambient particulate matter oxidative potential: chemical determinants, associated health effects, and strategies for risk management. Free Radic. Biol. Med. https://doi.org/10.1016/j.freeradbiomed.2020.04.028.

Ghio, A.J., 2004. Biological effects of Utah valley ambient air particles in humans: a review. J. Aerosol Med. 17 (2).

Goodman, M.M., Carling, G.T., Fernandez, D.P., Rey, K.A., Hale, C.A., Bickmore, B.R., Nelson, S.T., Munroe, J.S., 2019. Trace element chemistry of atmospheric deposition along the Wasatch Front (Utah, USA) reflects regional playa dust and local urban aerosols. Chem. Geol. 530 https://doi.org/10.1016/j.chemgeo.2019.119317.

Goudie, A.S., 2014. Desert dust and human health disorders. Environ. Int. https://doi.org/10.1016/j.envint.2013.10.011.

Hahnenberger, M., Nicoll, K., 2012. Meteorological characteristics of dust storm events in the eastern Great Basin of Utah, U.S.A. Atmos. Environ. 60, 601–612. https://doi.org/10.1016/j.atmosenv.2012.06.029.

Halliwell, B., 1992. Reactive Oxygen Species and the Central Nervous System. J. Neurochem. 59, 1609–1623. https://doi.org/10.1111/j.1471-4159.1992.tb10990.x.

Horne, B.D., Joy, E.A., Hofmann, M.G., Gesteland, P.H., Cannon, J.B., Lefler, J.S., Blagev, D.P., Kent Korgenski, E., Torosyan, N., Hansen, G.I., Kartchner, D., Arden Pope, C., 2018. Short-term elevation of fine particulate matter air pollution and acute lower respiratory infection. Am. J. Respir. Crit. Care Med. 198, 759–766. https://doi.org/10.1164/rccm.201709-1883OC.

Huang, J., Ji, M., Xie, Y., Wang, S., He, Y., Ran, J., 2016. Global semi-arid climate change over last 60 years. Clim. Dynam. 46, 1131–1150. https://doi.org/10.1007/s00382-015-2636-8.

Ichinose, T., Yoshida, S., Sadakane, K., Takano, H., Yanagisawa, R., Inoue, K., Nishikawa, M., Mori, I., Kawazato, H., Yasuda, A., Shibamoto, T., 2008. Effects of Asian sand dust, Arizona sand dust, amorphous silica and aluminum oxide on allergic inflammation in the murine lung. Inhal. Toxicol. 20 (7), 685–694. https://doi.org/10.1080/08958370801935133.

James Steenburgh, W., Massey, J.D., Painter, T.H., 2012. Episodic dust events of Utah's wasatch front and adjoining region. J. Appl. Meteorol. Climatol. 51, 1654–1669. https://doi.org/10.1175/JAMC-D-12-07.1.

Janssen, N.A.H., Yang, A., Strak, M., Steenhof, M., Hellack, B., Gerlofs-Nijland, M.E., Kuhlbusch, T., Kelly, F., Harrison, R., Brunekreef, B., Hoek, G., Cassee, F., 2014. Oxidative potential of particulate matter collected at sites with different source characteristics. Sci. Total Environ. 472, 572–581. https://doi.org/10.1016/j.scitotenv.2013.11.099.

Jayaratne, E.R., Johnson, G.R., McGarry, P., Cheung, H.C., Morawska, L., 2011. Characteristics of airborne ultrafine and coarse particles during the Australian dust

storm of 23 September 2009. Atmos. Environ. 45, 3996–4001. https://doi.org/10.1016/j.atmosenv.2011.04.059.
Jiang, Ahmed, Canchola, Chen, Lin, 2019. Use of Dithiothreitol Assay to Evaluate the Oxidative Potential of Atmospheric Aerosols. Atmosphere 10, 571. https://doi.org/10.3390/atmos10100571.
Jomova, K., Valko, M., 2011. Advances in metal-induced oxidative stress and human disease. Toxicology. https://doi.org/10.1016/j.tox.2011.03.001.
Jomova, K., Raptova, R., Alomar, S.Y., Alwasel, S.H., Nepovimova, E., Kuca, K., Valko, M., 2023. Reactive oxygen species, toxicity, oxidative stress, and antioxidants: chronic diseases and aging. Arch. Toxicol. https://doi.org/10.1007/s00204-023-03562-9.
Julien, C., Esperanza, P., Bruno, M., Alleman, L.Y., 2011. Development of an in vitro method to estimate lung bioaccessibility of metals from atmospheric particles. J. Environ. Monit. 13, 621–630. https://doi.org/10.1039/c0em00439a.
Kajino, M., Hagino, H., Fujitani, Y., Morikawa, T., Fukui, T., Onishi, K., Okuda, T., Igarashi, Y., 2021. Simulation of the transition metal-based cumulative oxidative potential in East Asia and its emission sources in Japan. Sci. Rep. 11 https://doi.org/10.1038/s41598-021-85894-z.
Kameda, T., Azumi, E., Fukushima, A., Tang, N., Matsuki, A., Kamiya, Y., Toriba, A., Hayakawa, K., 2016. Mineral dust aerosols promote the formation of toxic nitropolycyclic aromatic compounds. Sci. Rep. 6 https://doi.org/10.1038/srep24427.
Khansari, N., Shakiba, Y., Mahmoudi, M., 2009. Chronic Inflammation and Oxidative Stress as a Major Cause of Age- Related Diseases and Cancer. Recent Pat. Inflamm. Allergy Drug Discov. 3, 73–80. https://doi.org/10.2174/187221309787158371.
Kim, Hyo Jin, Herath, K.H.I.N.M., Dinh, D.T.T., Kim, H.S., Jeon, Y.J., Kim, Hyun Jung, Jee, Y., 2021. Sargassum horneri ethanol extract containing polyphenols attenuates PM-induced oxidative stress via ROS scavenging and transition metal chelation. J. Funct.Foods 79. https://doi.org/10.1016/j.jff.2021.104401.
Lang, O.I., Mallia, D., McKenzie Skiles, S., 2023. The shrinking Great Salt Lake contributes to record high dust-on-snow deposition in the Wasatch Mountains during the 2022 snowmelt season. Environ. Res. Lett. 18, 064045 https://doi.org/10.1088/1748-9326/acd409.
Lei, H., Wang, J.X.L., 2014. Observed characteristics of dust storm events over the western United States using meteorological, satellite, and air quality measurements. Atmos. Chem. Phys. 14, 7847–7857. https://doi.org/10.5194/acp-14-7847-2014.
Leiser, C.L., Smith, K.R., Vanderslice, J.A., Glotzbach, J.P., Farrell, T.W., Hanson, H.A., 2019. Evaluation of the sex-and-age-specific effects of PM2.5 on hospital readmission in the presence of the competing risk of mortality in the medicare population of utah 1999–2009. J. Clin. Med. 8 https://doi.org/10.3390/jcm8122114.
Levy, D.B., Schramke, J.A., Esposito, K.J., Erickson, T.A., Moore, J.C., 1999. The shallow ground water chemistry of arsenic, fluorine, and major elements: Eastern Owens Lake, California. Appl. Geochem. 14, 53–65. https://doi.org/10.1016/S0883-2927(98)00038-9.
Li, N., Hao, M., Phalen, R.F., Hinds, W.C., Nel, A.E., 2003. Particulate air pollutants and asthma: A paradigm for the role of oxidative stress in PM-induced adverse health effects. Clin. Immunol. https://doi.org/10.1016/j.clim.2003.08.006.
Lovett, C., Sowlat, M.H., Saliba, N.A., Shihadeh, A.L., Sioutas, C., 2018. Oxidative potential of ambient particulate matter in Beirut during Saharan and Arabian dust events. Atmos. Environ. 188, 34–42. https://doi.org/10.1016/j.atmosenv.2018.06.016.
Ma, X., Nie, D., Chen, M., Ge, P., Liu, Z., Ge, X., Li, Z., Gu, R., 2021. The relative contributions of different chemical components to the oxidative potential of ambient fine particles in nanjing area. Int. J. Environ. Res. Publ. Health 18, 1–17. https://doi.org/10.3390/ijerph18062789.
Malakootian, M., Mohammadi, A., Nasiri, A., Oliveri Conti, G., Faraji, M., 2022. Correlation between heavy metal concentration and oxidative potential of street dust. Air Qual Atmos Health 15, 731–738. https://doi.org/10.1007/s11869-021-01130-7.
Mallone, S., Stafoggia, M., Faustini, A., Paolo Gobbi, G., Marconi, A., Forastiere, F., 2011. Saharan dust and associations between particulate matter and daily mortality in Rome, Italy. Environ. Health Perspect. 119, 1409–1414. https://doi.org/10.1289/ehp.1003026.
Morman, S.A., Plumlee, G.S., 2013. The role of airborne mineral dusts in human disease. Aeolian Res. https://doi.org/10.1016/j.aeolia.2012.12.001.
Mudway, I.S., Duggan, S.T., Venkataraman, C., Habib, G., Kelly, F.J., Grigg, J., 2005. Combustion of dried animal dung as biofuel results in the generation of highly redox active fine particulates. Part. Fibre Toxicol. 2 https://doi.org/10.1186/1743-8977-2-6.
Murekhina, A.E., Yarullin, D.N., Sovina, M.A., Kitaev, P.A., Gamov, G.A., 2022. Copper (II)-Catalyzed Oxidation of Ascorbic Acid: Ionic Strength Effect and Analytical Use in Aqueous Solution. INORGA 10. https://doi.org/10.3390/inorganics10070102.
Nehra, A., Caplan, A.J., 2022. Nash bargaining in a general equilibrium framework: The case of a shared surface water supply. Water Resour Econ 39. https://doi.org/10.1016/j.wre.2022.100206.
Nishita-Hara, C., Hirabayashi, M., Hara, K., Yamazaki, A., Hayashi, M., 2019. Dithiothreitol-Measured Oxidative Potential of Size- Segregated Particulate Matter in Fukuoka, Japan: Effects of Asian Dust Events. Geohealth 3, 160–173. https://doi.org/10.1029/2019GH000189.
Nishita-Hara, C., Kobayashi, H., Hara, K., Hayashi, M., 2023. Dithiothreitol-Measured Oxidative Potential of Reference Materials of Mineral Dust: Implications for the Toxicity of Mineral Dust Aerosols in the Atmosphere. Geohealth. https://doi.org/10.1029/2022GH000736.
Ou, J., Pirozzi, C.S., Horne, B.D., Hanson, H.A., Kirchhoff, A.C., Mitchell, L.E., Coleman, N.C., Pope, C.A., 2020. Historic and modern air pollution studies conducted in utah. Atmosphere. https://doi.org/10.3390/atmos11101094.
Pant, P., Baker, S.J., Shukla, A., Maikawa, C., Godri Pollitt, K.J., Harrison, R.M., 2015. The PM10 fraction of road dust in the UK and India: Characterization, source profiles and oxidative potential. Sci. Total Environ. 530–531, 445–452. https://doi.org/10.1016/j.scitotenv.2015.05.084.
Pardo, M., Katra, I., Schaeur, J.J., Rudich, Y., 2017. Mitochondria-mediated oxidative stress induced by desert dust in rat alveolar macrophages. Geohealth 1, 4–16. https://doi.org/10.1002/2016GH000017.
Perrone, M.R., Bertoli, I., Romano, S., Russo, M., Rispoli, G., Pietrogrande, M.C., 2019. PM2.5 and PM10 oxidative potential at a Central Mediterranean Site: Contrasts between dithiothreitol- and ascorbic acid-measured values in relation with particle size and chemical composition. Atmos. Environ. 210, 143–155. https://doi.org/10.1016/j.atmosenv.2019.04.047.
Perry, K.D., Crosman, E.T., Hoch, S.W., Perry, K., 2019. Results of the Great Salt Lake Dust Plume Study Final Report.
Pietrogrande, M.C., Perrone, M.R., Manarini, F., Romano, S., Udisti, R., Becagli, S., 2018. PM10 oxidative potential at a Central Mediterranean Site: Association with chemical composition and meteorological parameters. Atmos. Environ. 188, 97–111. https://doi.org/10.1016/j.atmosenv.2018.06.013.
Pietrogrande, M.C., Russo, M., Zagatti, E., 2019. Review of PM oxidative potential measured with acellular assays in urban and rural sites across Italy. Atmosphere. https://doi.org/10.3390/atmos10100626.
Pietrogrande, M.C., Bacco, D., Trentini, A., Russo, M., 2021. Effect of filter extraction solvents on the measurement of the oxidative potential of airborne PM2.5. Environ. Sci. Pollut. Control Ser. 28, 29551–29563. https://doi.org/10.1007/s11356-021-12604-7.
Pope, C.A., Renlund, D.G., Kfoury, A.G., May, H.T., Horne, B.D., 2008. Relation of Heart Failure Hospitalization to Exposure to Fine Particulate Air Pollution. Am. J. Cardiol. 102, 1230–1234. https://doi.org/10.1016/j.amjcard.2008.06.044.
Putman, A.L., Jones, D.K., Blakowski, M.A., DiViesti, D., Hynek, S.A., Fernandez, D.P., Mendoza, D., 2022. Industrial Particulate Pollution and Historical Land Use Contribute Metals of Concern to Dust Deposited in Neighborhoods Along the Wasatch Front, UT, USA. Geohealth 6. https://doi.org/10.1029/2022GH000671.
Reynolds, R.L., Mordecai, J.S., Rosenbaum, J.G., Ketterer, M.E., Walsh, M.K., Moser, K. A., 2010. Compositional changes in sediments of subalpine Lakes, Uinta Mountains (Utah): Evidence for the effects of human activity on atmospheric dust inputs. J. Paleolimnol. 44, 161–175. https://doi.org/10.1007/s10933-009-9394-8.
Rodríguez-Cotto, R.I., Ortiz-Martínez, M.G., Jiménez-Vélez, B.D., 2015. Organic extracts from African dust storms stimulate oxidative stress and induce inflammatory responses in human lung cells through Nrf2 but not NF-κB. Environ. Toxicol. Pharmacol. 39, 845–856. https://doi.org/10.1016/j.etap.2015.02.015.
Rogers, L.K., Cismowski, M.J., 2018. Oxidative stress in the lung – The essential paradox. Curr Opin Toxicol 7, 37–43. https://doi.org/10.1016/j.cotox.2017.09.001.
Sauvain, J.J., Rossi, M.J., Riediker, M., 2013. Comparison of three acellular tests for assessing the oxidation potential of nanomaterials. Aerosol. Sci. Technol. 47, 218–227. https://doi.org/10.1080/02786826.2012.742951.
Schieber, M., Chandel, N.S., 2014. ROS function in redox signaling and oxidative stress. Curr. Biol. https://doi.org/10.1016/j.cub.2014.03.034.
Schweitzer, M.D., Calzadilla, A.S., Salamo, O., Sharifi, A., Kumar, N., Holt, G., Campos, M., Mirsaeidi, M., 2018. Lung health in era of climate change and dust storms. Environ. Res. 163, 36–42. https://doi.org/10.1016/j.envres.2018.02.001.
Shahpoury, P., Zhang, Z.W., Filippi, A., Hildmann, S., Lelieveld, S., Mashtakov, B., Patel, B.R., Traub, A., Umbrio, D., Wietzoreck, M., Wilson, J., Berkemeier, T., Celo, V., Dabek-Zlotorzynska, E., Evans, G., Harner, T., Kerman, K., Lammel, G., Noroozifar, M., Pöschl, U., Tong, H., 2022. Inter-comparison of oxidative potential metrics for airborne particles identifies differences between acellular chemical assays. Atmos. Pollut. Res. 13 https://doi.org/10.1016/j.apr.2022.101596.
Song, X.P., Hansen, M.C., Stehman, S.V., Potapov, P.V., Tyukavina, A., Vermote, E.F., Townshend, J.R., 2018. Global land change from 1982 to 2016. Nature 560, 639–643. https://doi.org/10.1038/s41586-018-0411-9.
Sosa, V., Moliné, T., Somoza, R., Paciucci, R., Kondoh, H., Lleonart, M.E., 2013. Oxidative stress and cancer: An overview. Ageing Res. Rev. https://doi.org/10.1016/j.arr.2012.10.004.
Stohs, S., 1995. Oxidative mechanisms in the toxicity of metal ions. Free Radic. Biol. Med. 18, 321–336. https://doi.org/10.1016/0891-5849(94)00159-H.
Thorsen, M.L., Handy, R.G., Sleeth, D.K., Thiese, M.S., Riches, N.O., 2017. A comparison study between previous and current shoreline concentrations of heavy metals at the Great Salt Lake using portable X-ray fluorescence analysis. Human and Ecological Risk Assessment 23, 1941–1954. https://doi.org/10.1080/10807039.2017.1349541.
Valavanidis, A., Fiotakis, K., Bakeas, E., Vlahogianni, T., 2005. Electron paramagnetic resonance study of the generation of reactive oxygen species catalysed by transition metals and quinoid redox cycling by inhalable ambient particulate matter. Redox Rep. 10, 37–51. https://doi.org/10.1179/135100005X21606.
Valko, M., Morris, H., Cronin, M., 2005. Metals, Toxicity and Oxidative Stress. Curr. Med. Chem. 12, 1161–1208. https://doi.org/10.2174/0929867053764635.
Valko, M., Jomova, K., Rhodes, C.J., Kuča, K., Musílek, K., 2016. Redox- and non-redox-metal-induced formation of free radicals and their role in human disease. Arch. Toxicol. https://doi.org/10.1007/s00204-015-1579-5.
Visentin, M., Pagnoni, A., Sarti, E., Pietrogrande, M.C., 2016a. Urban PM2.5 oxidative potential: Importance of chemical species and comparison of two spectrophotometric cell-free assays. Environ. Pollut. 219, 72–79. https://doi.org/10.1016/j.envpol.2016.09.047.

Visentin, M., Pagnoni, A., Sarti, E., Pietrogrande, M.C., 2016b. Urban PM2.5 oxidative potential: Importance of chemical species and comparison of two spectrophotometric cell-free assays. Environ. Pollut. 219, 72–79. https://doi.org/10.1016/j.envpol.2016.09.047.
Wurtsbaugh, W.A., 2012. Watershed Sciences Faculty Publications Watershed Sciences 3-2012 Paleominological Analysis of the History of Metals Contamination in the Great Salt Lake.
Wurtsbaugh, W.A., Sima, S., 2022. Contrasting management and fates of two sister lakes: Great Salt Lake (USA) and Lake Urmia (Iran). Water 14 (19), 3005. MDPI. https://doi.org/10.3390/w14193005.
Yadav, S., Phuleria, H.C., 2020. Oxidative Potential of Particulate Matter. A Prospective Measure to Assess PM Toxicity 333–356. https://doi.org/10.1007/978-981-15-0540-9_16.
Yang, A., Wang, M., Eeftens, M., Beelen, R., Dons, E., Leseman, D.L.A.C., Brunekreef, B., Cassee, F.R., Janssen, N.A.H., Hoek, G., 2015. Spatial variation and land use regression modeling of the oxidative potential of fine particles. Environ. Health Perspect. 123, 1187–1192. https://doi.org/10.1289/ehp.1408916.
Yu, Y., Zou, W., Jerrett, M., Meng, Y.Y., 2023. Acute health impact of wildfire-related and conventional PM2.5 in the United States: A narrative review. Environmental Advances. https://doi.org/10.1016/j.envadv.2022.100179.
Zhang, X., Zhao, L., Tong, D.Q., Wu, G., Dan, M., Teng, B., 2016. A systematic review of global desert dust and associated human health effects. Atmosphere. https://doi.org/10.3390/atmos7120158.